We are IntechOpen, the world's leading publisher of Open Access books Built by scientists, for scientists

4,800
Open access books available

122,000
International authors and editors

135M
Downloads

Our authors are among the

154
Countries delivered to

TOP 1%
most cited scientists

12.2%
Contributors from top 500 universities

CLARIVATE ANALYTICS BOOK CITATION INDEX INDEXED

WEB OF SCIENCE™

Selection of our books indexed in the Book Citation Index in Web of Science™ Core Collection (BKCI)

Interested in publishing with us?
Contact book.department@intechopen.com

Numbers displayed above are based on latest data collected.
For more information visit www.intechopen.com

Chapter 12

Photo-Catalytic Degradation of Volatile Organic Compounds (VOCs) over Titanium Dioxide Thin Film

Wenjun Liang, Jian Li and Hong He

Additional information is available at the end of the chapter

http://dx.doi.org/10.5772/48099

1. Introduction

Volatile organic compounds (VOCs) are emitted as gases from certain solids or liquids. VOCs include a variety of chemicals, some of which may have short- and long-term adverse health effects. Concentrations of many VOCs are consistently higher indoors (up to ten times higher) than outdoors.

The control of VOCs in the atmosphere is a major environmental problem. The traditional methods of VOCs removal such as absorption, adsorption, or incineration, which are referred to the new environmental condition have many technical and economical disadvantages. So in recent years, some new technologies called advanced oxidation processes (AOPs), such as biological process, photo-catalysis process or plasma technology, are paid more and more attention.

Advanced oxidation processes (AOPs) are efficient novel methods useful to accelerate the non-selective oxidation and thus the destruction of a wide range of organic substances resistant to conventional technologies. AOPs are based on physicochemical processes that produce in situ powerful transitory species, principally hydroxyl radicals, by using chemical and/or other forms of energy, and have a high efficiency for organic matter oxidation.

Among AOPs, photocatalysis has demonstrated to be very effective to treat pollutants both in gas and in liquid phase. The photo-excitation of semiconductor particles (TiO_2) promotes an electron from the valence band to the conduction band thus leaving an electron deficiency or hole in the valence band; in this way, electron/hole pairs are generated. Both reductive and oxidative processes can occur at/or near the surface of the photo-excited semiconductor particle.

Photocatalytic degradation of VOCs on UV-illuminated titanium dioxide (TiO_2) is proposed as an alternative advanced oxidation process for the purification of water and air. Heterogeneous photo-catalysis using TiO_2 has several attractions: TiO_2 is relatively inexpensive, it dispenses with the use of other coadjutant reagents, it shows efficient destruction of toxic contaminants, it operates at ambient temperature and pressure, and the reaction products are usually CO_2 and H_2O, or HCl, in the case of chlorinated organic compounds. Decomposition path of VOCs with UV/TiO_2 or UV/TiO_2/doped ions is shown in Fig. 1. However, the formations of by-products, such as CO, carbonic acid and coke-like substances, were often observed. These by-product formations are due to low degradation rate of intermediate compounds that are formed by the partial oxidation of VOCs. In order to improve the VOC degradation rate, some authors reported on the enhancement of VOC degradation through the addition of anions (dopant = S, N, P, etc), cations (dopant = Pt, Cu, Mg, etc), polymers or co-doped with several ions on TiO_2, while the difference between doping agents has not been discussed yet.

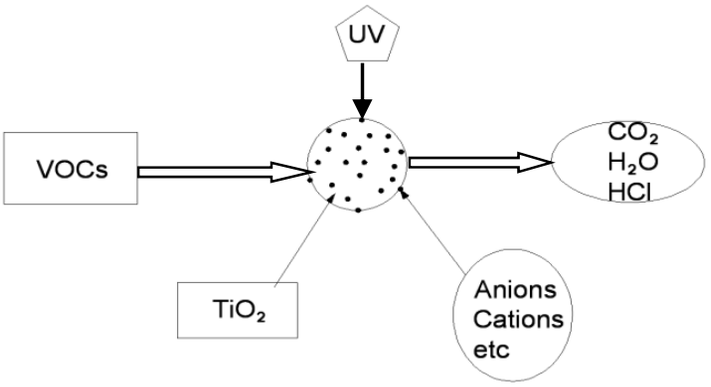

Figure 1. Decomposition path of VOCs with UV/TiO_2.

In this chapter, toluene, p-xylene, acetone and formaldehyde were chosen as the model VOCs because they were regarded as representative indoor VOCs for determining the effectiveness and capacity of gas-phase air filtration equipment for indoor air applications, the photo-catalytic degradation characters of them by TiO_2/UV, TiO_2/doped Ag/UV and TiO_2/doped Ce/UV was tested and compared. The effects of hydrogen peroxide, initial concentration, gas temperature, relative humidity of air stream, oxygen concentration, gas flow rate, UV light wavelength and photo-catalyst amount on decomposition of the pollutants by TiO_2/UV were analyzed simultaneously. Furthermore, the mechanism of titania-assisted photo-catalytic degradation was analyzed, and the end product of the reaction using GC-MS analysis was also performed.

2. Materials and methods

2.1. Chemicals and experimental set-up

Acetone, toluene, p-xylene and formaldehyde used in our experiment was analytical reagent. The TiO_2 photocatalyst was prepared with 100 % anatase using the sol-gel method,

and immobilized as a film (thickness 0.2 mm) on glass springs. Ethanol, tetrabutyl orthotitanate, diethanolamine, N,N-dimethylformamide and polyethylene glycol used as raw materials for photocatalyst preparation were of analytical grade and utilized without further purification. $AgNO_3$, $Ce(NO_3)_3 \bullet 6H_2O$ were used as Ag or Ce source for modified TiO_2 samples. Deionized water was used throughout the study.

A schematic diagram of the experimental system for photo-oxidation is shown in Fig. 2. The experiments were performed in a cylindrical photo-catalytic reactor with inner diameter 18.0 mm. A germicidal lamp (wavelength range 200-300 nm) with the maximum light intensity at 254 nm was installed in the open central region. The desired amount of representative sample, that is acetone, toluene, p-xylene or formaldehyde, was injected into the obturator. Then, the photo-catalytic degradation was performed by transporting the gas across the photo-catalyst continuously when UV lamp was turned on. Glass spring coated by a TiO_2 thin film was filled around the lamp. In whole experiment, humidity was controlled and adjusted with vapour. In some experiments it was replaced with a 15 W black-light lamp with a maximum light intensity output at 365 nm. After a stabilized period of about 3 h, the pollutant concentrations in the outlet gas became the same as in the inlet gas, and the experiment was started by turning on the UV lamp. Relative humidity of the reactor was detected with humidity meter. Oxygen concentration was controlled with oxygen detector.

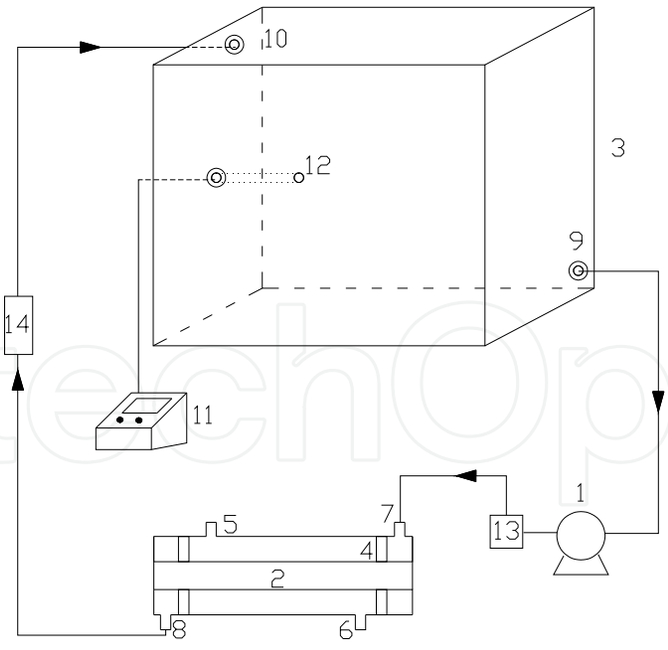

Figure 2. Schematic diagram of experimental set-up. 1- Minitype circulation pump; 2 - Germicidal lamp; 3 - Obturator (airproof tank, 125 L); 4 - Lacunaris clapboard; 5, 6 - Sampling spots; 7-10 – Inlet & Outlet; 11 - Temperature-humidity detector; 12 - Probe; 13 - Gas heated container; 14 - Humidity controller.

2.2. Photo-catalyst preparation

Fig. 3 shows the schematic flow-chart of the experimental procedure.TiO_2 precursor sols were prepared by adding tetrabutylorthotitanate (400 mL) into ethanol (960 mL) at room temperature. Then diethanolamine (69.1 mL) was added, and the mixture stirred for 2 hr. Subsequently, ethanol (120 mL), deionized water (25.2 g), 5 wt% $AgNO_3$ or $Ce(NO_3)_3$ were added dropwise to the solution. After stirring for 15 min, N,N-dimethylformamide (16.8 mL) was added. This reduced surface tension and made a smooth coating of the thin film on the carrier. The solution was then left to rest for 24 hr. Finally, polyethylene glycol (4.32 g) dissolved in ethanol (120 mL) at 50 °C was added dropwise to the solution. The final solution was left to sit for 12 hr, after which the TiO_2 gel had formed. The prepared mixture could remain stable for months at ambient temperature. Thin film TiO_2 photocatalyst was formed by dip-coating with a velocity of 5 cm/s. Glass springs were selected as the photocatalyst carrier due to their excellent transparency and long light diffusion distance. Fig. 4 was the sketch of glass spring structure. These were immersed in the TiO_2 gel mixture, and then dried at room temperature. This was followed by calcination at 500 °C in a muffle furnace for 2 hr. The glass springs were coated repeatedly (total of five times) using this method to form a thin TiO_2 photocatalyst film. The TiO_2 film was very stable and durable, and no loss was observed during its application.

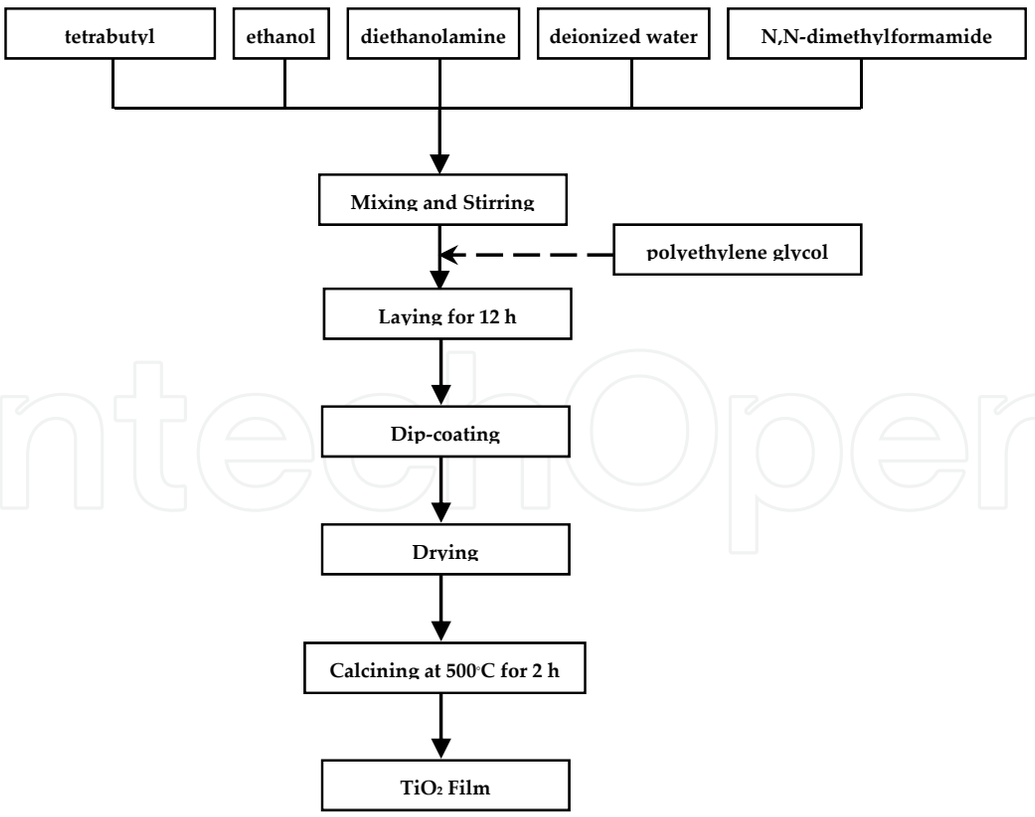

Figure 3. Flowchart of photo-catalyst preparation.

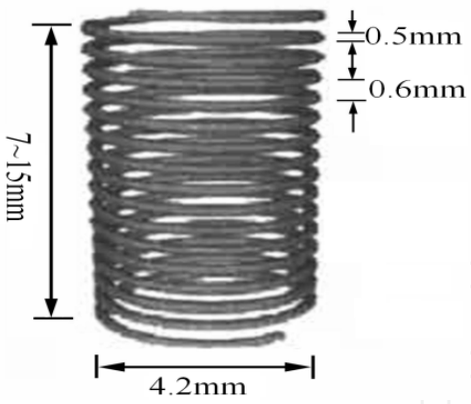

Figure 4. Sketch of glass spring structure.

2.3. Analytical methods

The concentrations of acetone, toluene, and p-xylene were analyzed by a gas chromatograph (Model GC-14C, Shimadzu, Japan) with a flame ionization detector (FID). The oven temperature was held at 60 °C and detector temperature maintained constant at 100 °C. The end products of the reaction were detected by GC-MS. GC-MS analysis was conducted using an HP 6890N GC and HP 5973i MSD. A HP-5 capillary column (30m×0.32mm ID) was used isothermally at 60 °C. The carrier gas (helium) flow-rate was 30 cm/s, and the injector and detector temperatures were 150°C and 280°C, respectively. Intermediate products analysis was done by EI mode and full scan. Formaldehyde concentration in gas stream was determined by acetylacetone spectrophotometric method. HCHO absorbed by deionized water in acetic acideammonium acetate solution would react with acetylacetone to form a steady yellow compound. HCHO concentration in the gas stream was then determined by measuring light absorbance at 413 nm with a spectrophotometer (UV/Vis 722). Temperature and humidity were measured with a temperature-humidity detector (Model LZB-10WB, Beijing Yijie Automatic Equipment Ltd., China).

The characteristics of the immobilized nano-structured TiO_2 thin film were analyzed by field-emission scanning electron microscopy (FE-SEM, Model JSM 6700F, JEOL, Japan) and X-ray diffractometry (XRD, Rigaku, D-max-γA XRD with Cu Kα radiation, λ = 1.54178 Å). The surface area of the TiO_2 film was also analyzed using gas adsorption principles (Detected by Micromeritics, American Quantachrome Co., NOVA 1000). The synthesized samples had a BET surface area of 56.3 m^2/g, compared with Degussa P25 TiO_2 with a surface area of 50.2 m^2/g.

The degradation rates (%) of acetone, toluene, p-xylene and formaldehyde were calculated as follows:

$$\eta = \frac{C_i - C_o}{C_i} \times 100\% \quad (1)$$

where C_i is the inlet concentration, and C_o is the outlet concentration at steady state.

3. Results and discussion

3.1. SEM and XRD Images of the Photocatalyst

FE-SEM analysis of the particle size and shape of the synthesized TiO_2 sample showed it consisted of uniform nano-particles (Fig. 5). However, some cracks were found on the surface. A major contributor to these cracks could be the greater surface tension resulting from the small diameter (0.5 mm) of the glass springs and the high-temperature sintering process. In further experiments, we decreased the temperature from 500 °C to 450 °C. At the lower temperature, there were fewer cracks on the surface but they were not eliminated completely.

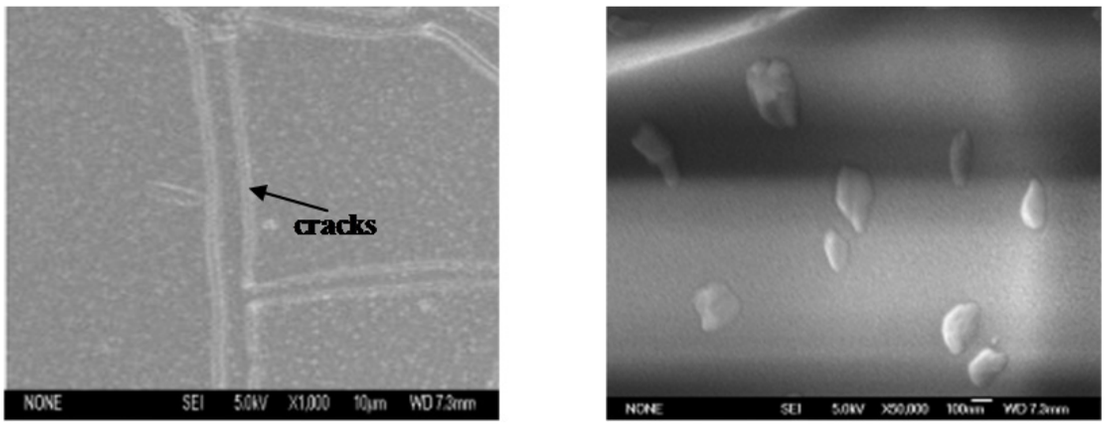

Figure 5. SEM photographs and macroscopic morphology of the TiO_2 thin film coated on a glass spring.

The left and right photographs were taken at 1000× and 50 000× magnification, respectively.

According to Scherrer's equation (Eq. 2) and XRD patterns, the particle size of TiO_2 (D) was calculated to be 35 nm.

$$D = k\lambda / \beta \cos\theta \tag{2}$$

The crystalline phase of the TiO_2 catalyst was analyzed by XRD (Fig. 6). All the diffraction peaks in the XRD pattern could be assigned to tetragonal anatase TiO_2, with lattice constants of a=0.3785 nm, b=0.3785 nm, and c=0.9514 nm.

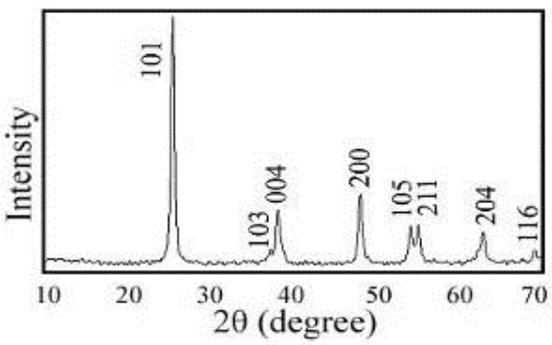

Figure 6. XRD spectrum of anatase crystalline phase of the TiO_2 catalyst

3.2. Effect of doped Ag/TiO_2 or Ce/TiO_2 on decomposition of VOCs

The characters of catalyst are important for the degradation of VOCs. Fig. 7 illustrates the degradation rates of acetone, toluene, and p-xylene (ATP) as functions of irradiation time when pure TiO_2, Ag-TiO_2 and Ce–TiO_2 were used. As controls, blank experiments in the absence of TiO_2 had been studied. The results corresponded to the flow-rate of 1 L/min, initial concentration of 0.1 mol/m^3 and relative humidity of 35%. It was found that all the conversions of ATP in the TiO_2/UV, Ag-TiO_2/UV and Ce-TiO_2/UV processes were increased with irradiation time. Table 1 shows the degradation rates for both catalysts after 8-h photo-catalytic reaction. It can be seen from Fig. 7 and Table 1 that the doping of silver or cerium ions could improve the photo-activity of TiO_2 effectively. Furthermore, the degradation character of the photo-catalyst was in the order Ce-TiO_2 > Ag-TiO_2 > TiO_2. Besides, the results of blank experiments in the absence of TiO_2 showed that the removal efficiency of ATP was very low. For example, the removal efficiency of acetone was merely 6.3% after 8 h and lower than 46.5% for pure TiO_2, which means that TiO_2 plays an important role in photo-catalytic reaction.

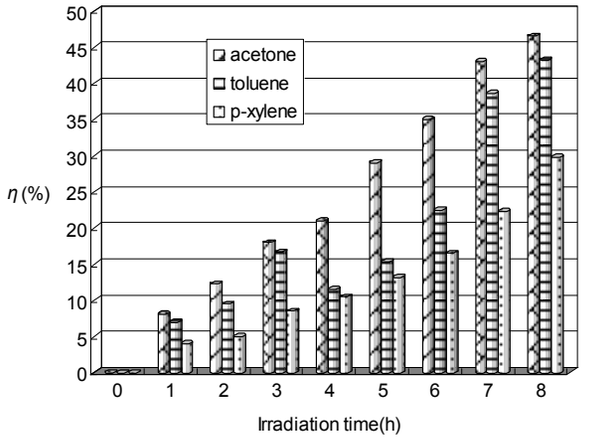

(TiO_2)

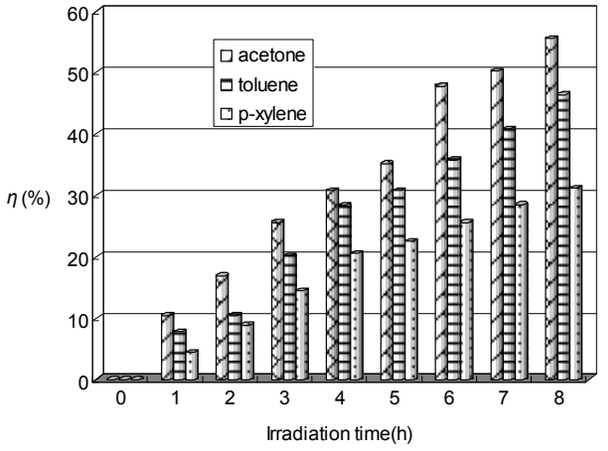

(Ag-TiO_2, 5wt%)

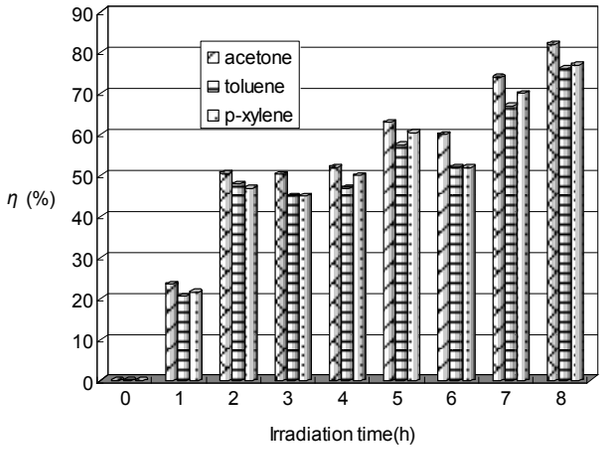

(Ce-TiO_2, 5wt%)

Figure 7. Effect of doped Ag/Ce/TiO_2 on decomposition of ATP.

Catalyst	TiO_2	Ag-TiO_2	Ce-TiO_2
η (acetone, %)	46.5	55.5	82.0
η(toluene, %)	43.2	46.4	76.2
η (*p*-xylene, %)	29.8	31.2	77.8

Table 1. ATP degradation rates for different catalysts after 8 hrs.

Fig. 8 illustrated the effect of doped Ag/Ce/TiO_2 on decomposition of HCHO. The conditions were as follows: flow-rate of 3 L/min, initial concentration of 0.1 mg/m^3, relative humidity of 35%. It was found that conversions of HCHO in the TiO_2/UV, Ag-TiO_2/UV and Ce-TiO_2/UV processes were increased with irradiation time. It could be seen that the doping of silver or cerium ions could improve the photo-activity of TiO_2 effectively. Furthermore, the degradation character of the photo-catalyst was in the order Ce-TiO_2 > Ag-TiO_2 > TiO_2.

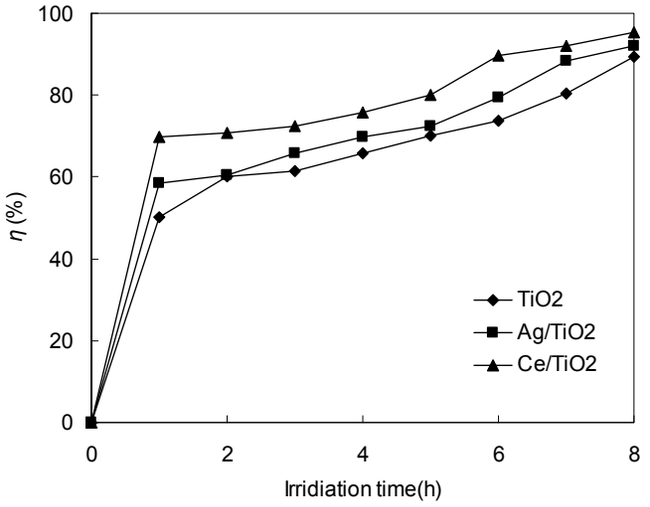

Figure 8. Effect of doped Ag/Ce/TiO_2 on decomposition of HCHO.

The reason was as follows: Ag/Ce doping could narrow the band gap. The narrower band gap will facilitate excitation of an electron from the valence band to the conduction band in the doped TiO_2, thus increasing the photo-catalytic activity of the material. At the same time, silver or cerium species could create a charge imbalance, vacancies and unsaturated chemical bonds on the catalyst surface. It will lead to the increase of chemisorbed oxygen on the surface. Surface chemisorbed oxygen has been reported to be the most active oxygen, and plays an important role in oxidation reaction. Herein, silver or cerium modified TiO_2 might have better activity for the oxidation of VOCs. Furthermore, samples after Ag/Ce doping treatment showed a slight change of colour from white to yellowish.

The photo-catalytic activity of Ce-TiO_2 in the oxidative degradation of VOCs being higher than that of Ag-TiO_2 may be explained as follows: Compared to Ag, Ce doping serves as an electron trap in the reaction because of its varied valences and special 4f level. For Ce^{3+}-TiO_2, the Ce 4 f level plays an important role in interfacial charge transfer and elimination of electron-hole recombination. So, Ce doping could enhance the electron-hole separation and the decomposition rate of VOCs could be elevated. Moreover, the valence electrons of TiO_2 catalyst are excited to the conduction band by UV light, and after various other events, electrons on the TiO_2 particle surface are scavenged by the molecular oxygen to produce reactive oxygen radicals. Furthermore, redox reactions between the pollutant molecules and reactive oxygen radicals happened, VOC molecules were turned into harmless inorganic compounds, such as CO_2 and H_2O at the end.

3.3. Effect of Hydrogen Peroxide

Hydrogen peroxide is considered to have two functions in the photo-catalytic degradation. It accepts a photo-generated conduction band electron, thus promoting the charge separation, and it also forms OH•. The addition of H_2O_2 increases the concentration of OH• radicals since it inhibits the electron-hole recombination.

Experiments were conducted to evaluate the effect of H_2O_2 on the toluene/p-xylene photo-degradation. The conditions were as follows: flow rate of 1 L/min, initial concentration of 0.1 mol/m^3, relative humidity of 35%, and photo-catalyst of pure TiO_2. As shown in Fig. 9, the removal efficiency of toluene or p-xylene increased with reaction time.

In the first 3 h, the degradation rate of toluene or p-xylene without H_2O_2 was higher because of the competitive adsorption between toluene or p-xylene molecules and hydrogen peroxide. Then, more reactants and/or radical molecules were produced during the photo-chemistry course, which led to the improvement of toluene or p-xylene decomposition. The final degradation rates of toluene and p-xylene with H_2O_2 were up to 97.1 and 95.4% after 8 h, respectively.

The degradation of acetone was studied with and without hydrogen peroxide (Fig. 10). Overall, the acetone removal efficiency increased with reaction time. Initially, the degradation rate of without H_2O_2 was higher than that of with H_2O_2 because of competitive adsorption between acetone and hydrogen peroxide after hydrogen peroxide addition to the

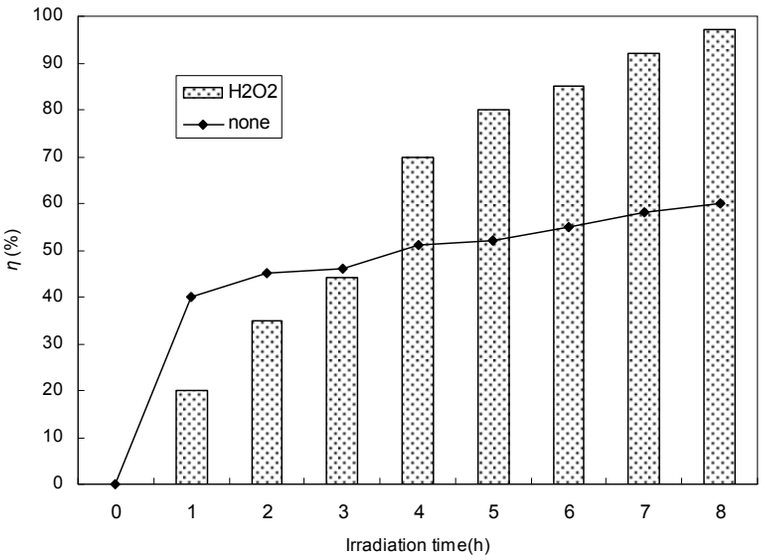

(Toluene)

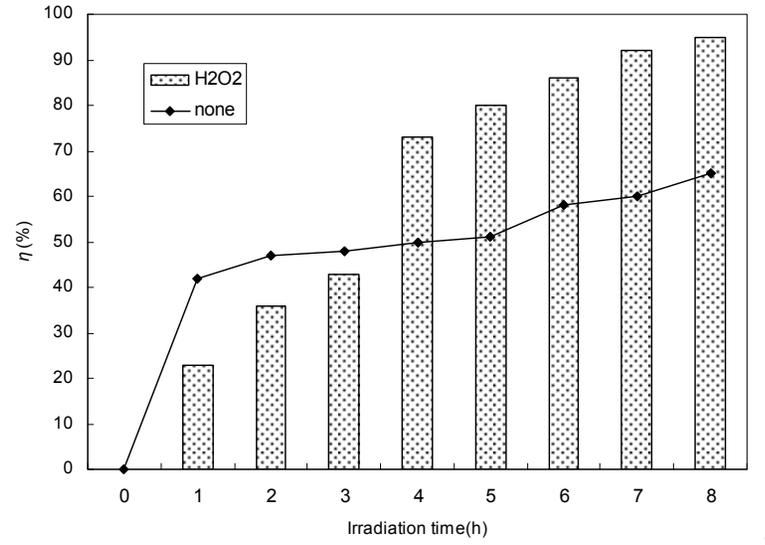

(*P*-xylene)

Figure 9. Effect of toluene/p-xylene degradation on hydrogen peroxide.

sample chamber (10 mL per 30 min, 30 % H_2O_2, RH 35 %). As the reactants and/or byproducts accumulated on the catalyst, and there was no new super-oxidation supplied, the catalyst deactivated and the degradation rate increased slowly after 2 hr. Hydroxyl radicals were produced due to the presence of hydrogen peroxide (Eq. 3). This decreased recombination of electron-hole pairs, and consequently the final acetone degradation rate was up to 91.8 % after 8 hr. Consumption of hydroxyl radical likely played an important role in deactivation of the catalyst. An appropriate volume of hydrogen peroxide could enhance the degradation rate, while too much could decrease the degradation rate (Eq. 4).

$$H_2O_2 + e^- \rightarrow \cdot OH + OH^- \quad (3)$$

$$H_2O_2 + \cdot OH \rightarrow H_2O + HO_2 \cdot \quad (4)$$

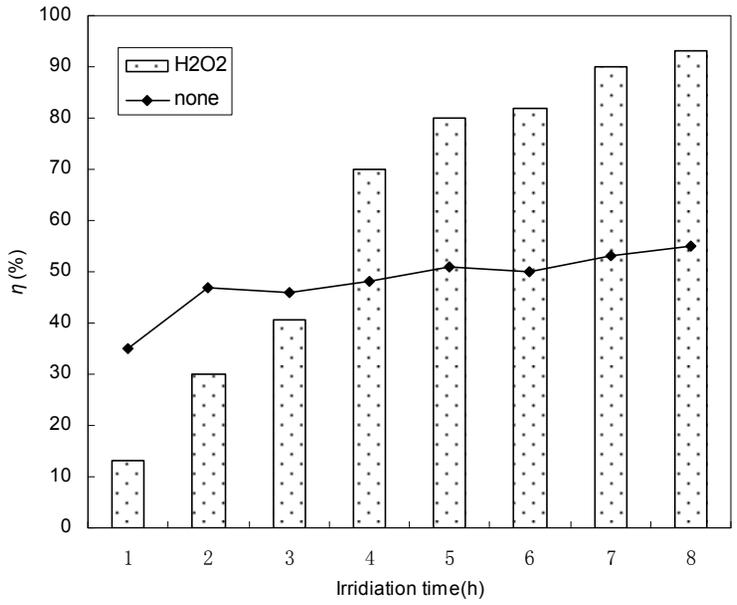

Figure 10. Effect of acetone degradation on hydrogen peroxide.

During deactivation the catalyst color in process without H_2O_2 changed from light white to khaki, while with H_2O_2 was light khaki. This suggests catalyst deactivation in process without H_2O_2 was more extensive than in with H_2O_2. Moreover, the change in catalyst color after the reaction indicates that the reaction occurred in the surface of the catalyst. After sintering at 390 °C for 1 h the catalyst recovered its original color. This again suggests that catalyst deactivation was due to the accumulation of reactants and by-products on the catalyst surface, which impeded degradation reactions. To compare the performance of H_2O_2/UV, we evaluated the potential of acetone degradation by H_2O_2 alone. The concentration of acetone remained almost the same over 8 h. Consequently, we concluded that H_2O_2 alone could not remove the VOCs.

3.4. Effect of initial concentration

In order to discuss the effect of VOCs initial concentration on photo-catalytic degradation rates, we investigated the removal efficiency of ATP and HCHO under different initial concentrations. The ATP concentrations in the experiment ranged between 0.05-0.3 mol/m^3. The conditions were as follows: gas flow-rate of 1 L/min, relative humidity of 35%, Ce-doped TiO_2 as photo-catalyst, and irradiation time of 8 hr. The results showed that the photo-catalytic degradation rates decreased with increasing ATP initial concentration, just illustrated in Fig. 11. Based on the Langmuir-Hinshelwood equation, the degradation rate decreased with increasing initial concentration while the absolute amount of degraded

pollutants may increase. At higher initial concentration, the UV light might be absorbed by gaseous pollutants rather than the TiO_2 particles, which led to the reduction of the photo-degradation efficiency. Moreover, at different initial concentrations, acetone was easiest to be destructed, while p-xylene was difficult to be removed among ATP from gas flow.

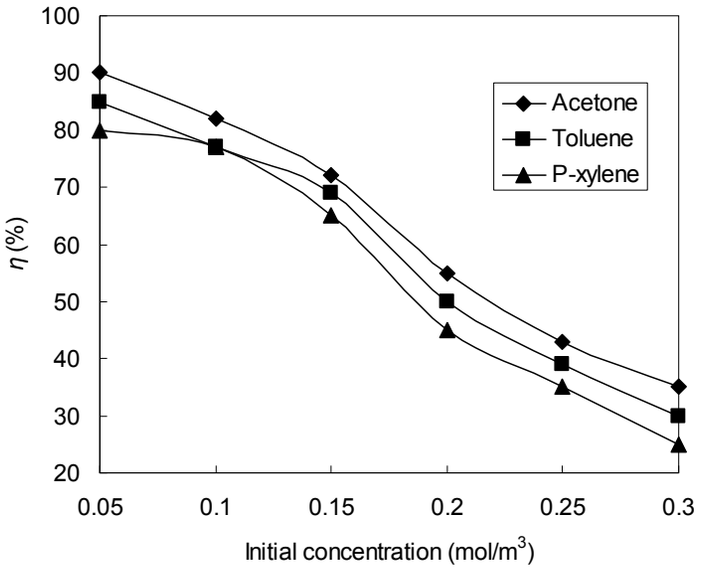

Figure 11. Effect of ATP initial concentration on the photo-catalysis of ATP by TiO_2.

As a main indoor pollutant, the indoor formaldehyde concentration is usually below 0.5 ppmv. It is worth discussing whether the low level of indoor HCHO can be decreased to a value below 0.1 mg/m^3 (specified in the indoor air quality standard of China). So in our experiment, the HCHO concentrations in the experiment ranged between 0.1-0.5 mg/m^3. The conditions were as follows: relative humidity of 35%, Ce-doped TiO_2 as photo-catalyst, and irradiation time of 120min. The results showed that the photo-catalytic degradation rates decreased with increasing HCHO initial concentration, just illustrated in Fig. 12.

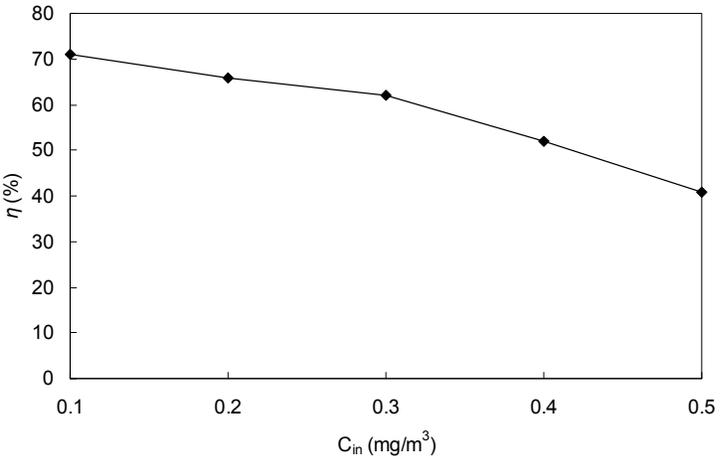

Figure 12. Effect of initial HCHO concentration on HCHO degradation by TiO_2.

In gas-phase photo-catalyst, collision frequency between radicals and HCHO affected the removal efficiency. When formaldehyde molecule reaches to the catalyst surface, the photo oxidation will occur. At higher initial concentration, the UV light might be absorbed by gaseous pollutants rather than the TiO_2 particles, which led to the reduction of the photo-degradation efficiency.

3.5. Effect of UV Light Wavelength

In order to investigate the influence of the UV intensity on the photo-catalytic efficiency, the experiments were performed using two lamp configurations (254 and 365 nm). The effect of UV light wavelength on the efficiency of HCHO degradation is shown in Fig. 13. Just shown in Fig.13, 254 nm UV light provided more effective HCHO photo-degradation than 365 nm UV light.

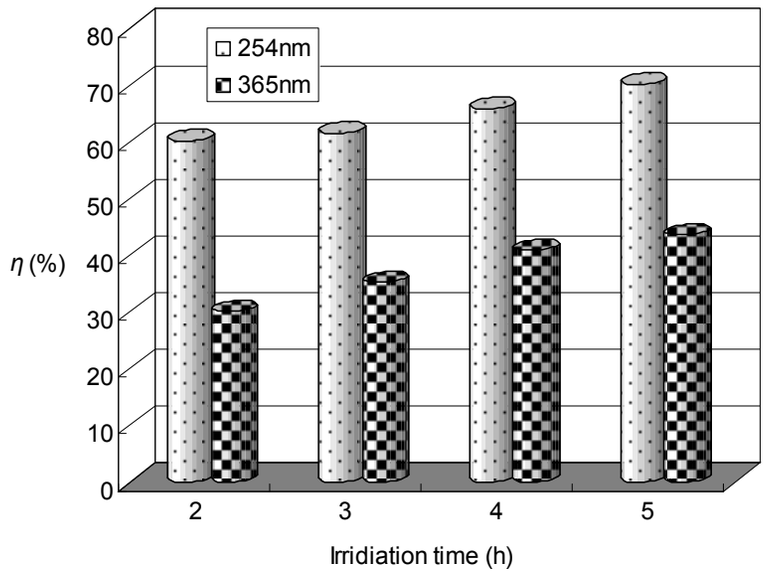

Figure 13. Effect of UV light wavelength on HCHO degradation.

The effect of UV light wavelength on the efficiency of ATP degradation is shown in Fig.14. 254 nm UV light provided more effective ATP photodegradation than 365 nm UV light. Degradation of ATP in the UV/TiO_2 process followed the same trend.

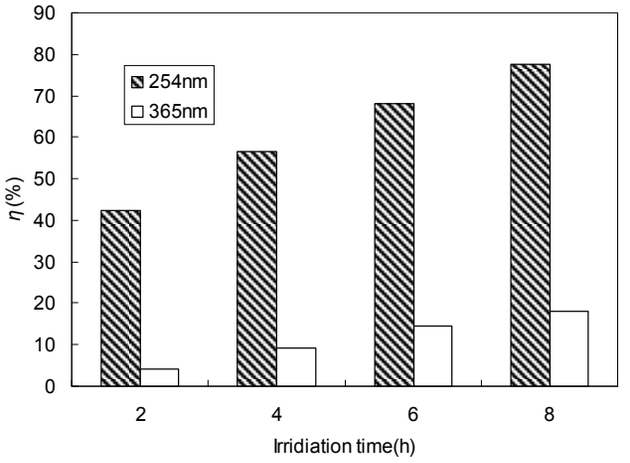

(a) Acetone

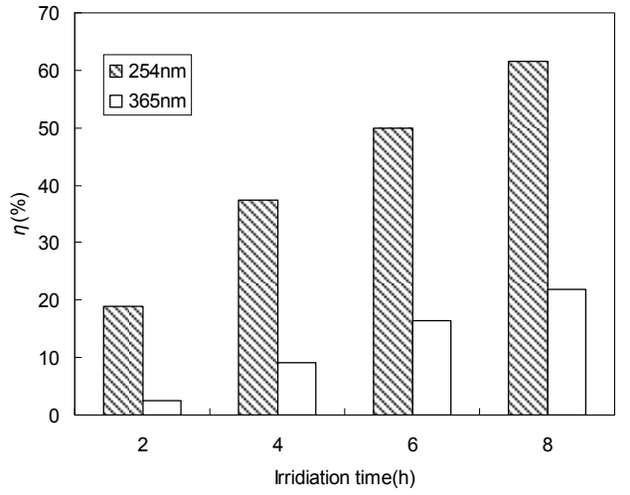

(b) Toluene

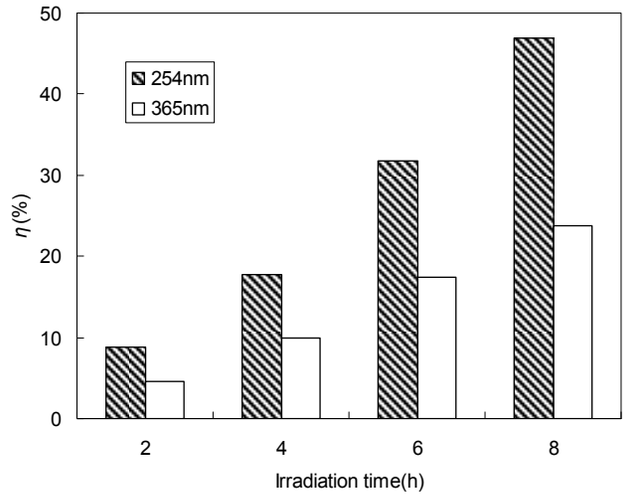

(c) P-xylene

Figure 14. Effect of UV wavelength on degradation of acetone, toluene, and p-xylene by TiO_2/UV processes.

The different results obtained with 254 and 365 nm UV lamps were mainly due to the stronger UV irradiation from the 254 nm lamp (about 58 W/m^2 on its surface) than that from the 365 nm lamp (30 W/m^2 on its surface). This illustrates that the 254 nm UV lamp irradiated photons with higher energy, which led to more efficient degradation with TiO_2/UV.

3.6. Effect of gas flow rate

The effect of gas flow rate on ATP degradation was studied at an initial concentration of 0.1 mol/m^3 and relative humidity of 35 %, just as shown in Fig. 15. When the flow rate was increased from 3–9 L/min, degradation of toluene and acetone decreased. With a flow rate >3 L/min the reactants have shorter residence time on the photocatalyst surface and consequently do not bind to the active sites. In general, an increase in gas flow rate results in two antagonistic effects. These are a decrease in residence time within the photocatalytic reactor, and an increase in the mass transfer rate. In our opinion, the decrease in degradation with increasing gas flow rate showed that the residence time of pollutant molecules with TiO_2 is an important factor. However, the degradation rate at 1 L/min was the lowest. This was due to adsorption of active species on the catalyst, which led to a decrease in the reaction between pollutant molecules and active species. For p-xylene, the degradation rate was the highest when the flow rate was 7 L/min. From these results it can be concluded that gas flow rate remarkably influences the degradation rate. While both toluene and p-xylene are aromatic hydrocarbons, toluene is an unsymmetrical molecule and p-xylene is symmetrical. Consequently, the adsorption and degradation of toluene were greater than for p-xylene under the same flow rate. The highest degradation rates for acetone, toluene, and p-xylene were 77.7, 61.9, and 55 %, respectively.

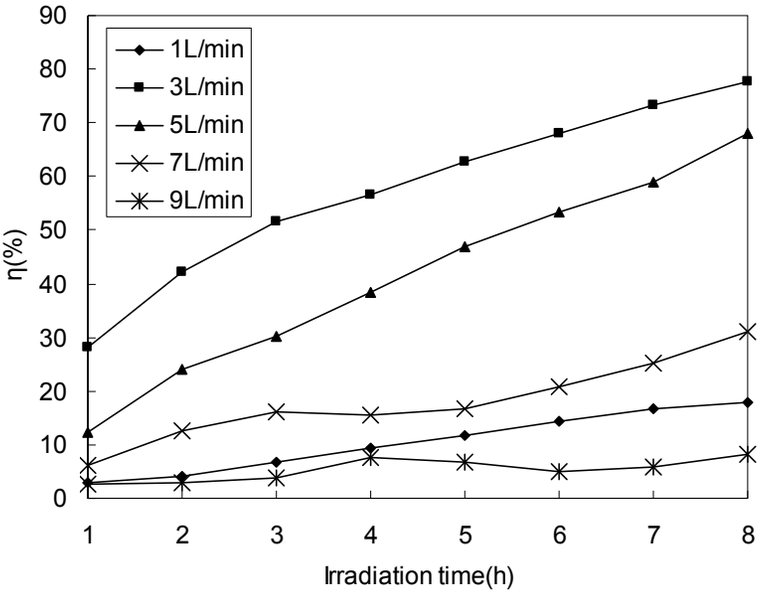

(a) Acetone

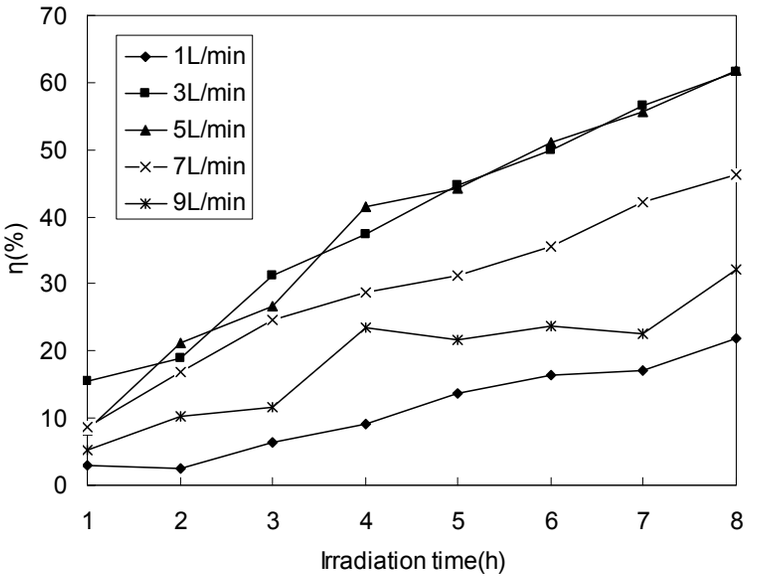

(b) Toluene

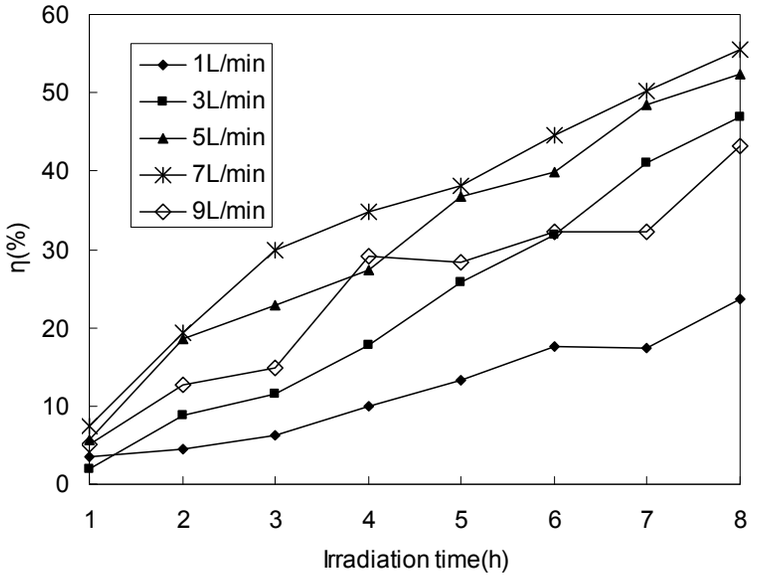

(c) P-xylene

Figure 15. Effect of flow rate on the degradation of acetone, toluene, and p-xylene by TiO_2/UV processes.

The Langmuir–Hinshelwood (L–H) rate expression has been widely used to describe the gas–solid phase reaction for heterogeneous photocatalysis. Assuming that mass transfer is not the limiting step, and that the effect of intermediate products is negligible, then the reaction rate in a plug-flow reactor can be expressed as:

$$r = -\frac{dC_{VOC}}{dt} = \frac{kKC}{1+KC} \tag{5}$$

where k and K are the L–H reaction rate constant and the L–H adsorption equilibrium constant, respectively; and t is the time taken for ATP molecules to pass through the reactor. After integration of Equation (5) the following linear expression can be obtained:

$$\frac{\ln(C_{in}/C_{out})}{(C_{in}-C_{out})} = \frac{kKT}{(C_{in}-C_{out})} - K \tag{6}$$

where C_{in} and C_{out} are the inlet and outlet concentrations of ATP, respectively; and T is the recurrent time of VOCs in the reactor.

If the L–H model is valid, a plot of $ln(C_{in}/C_{out})/(C_{in}-C_{out})$ versus $1/(C_{in}-C_{out})$ should be linear. This was the case with our data (Fig. 16), and the linearity correlation coefficients of acetone, toluene and p-xylene were 0.9989, 0.9995 and 0.9992, respectively. This result suggests that the reaction occurs on the photocatalyst surface through an L–H mechanism and not in the gas phase.

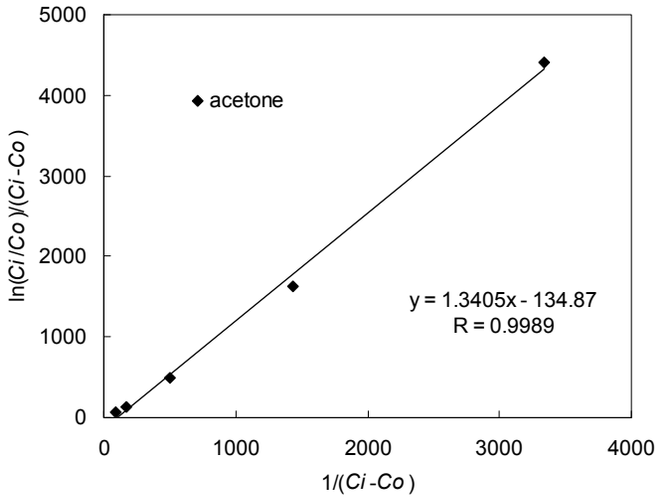

(a) Acetone

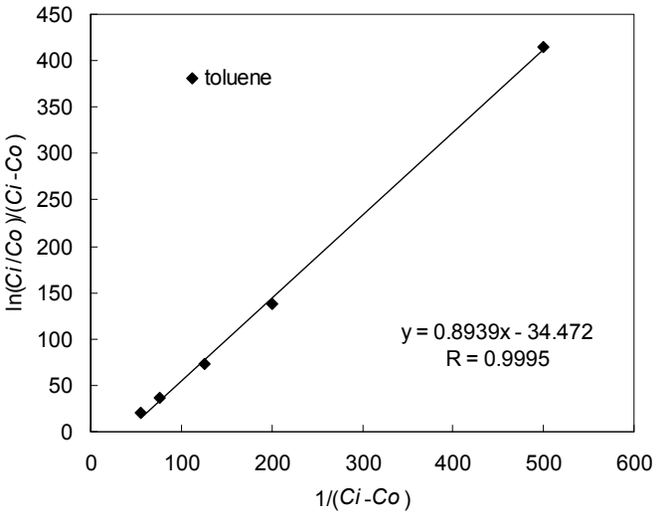

(b) Toluene

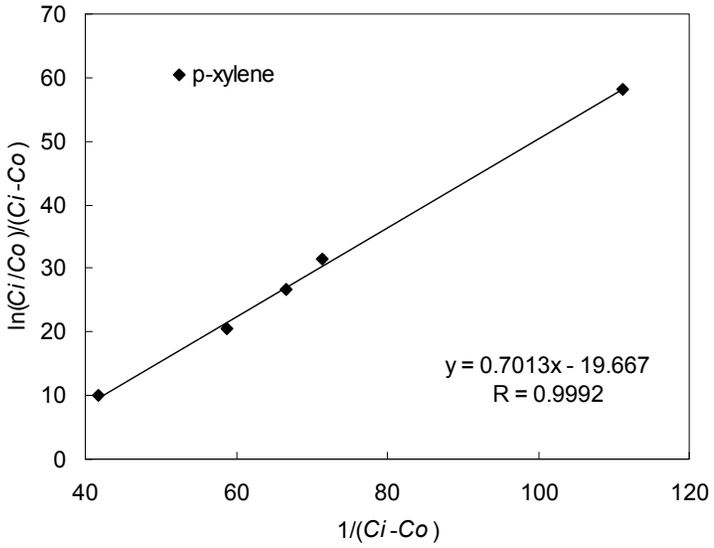

(c) P-xylene

Figure 16. Plot of $\ln(C_{in}/C_{out})/(C_{in}-C_{out})$ and $1/(C_{in}-C_{out})$.

3.7. Degradation of Pure Individual VOCs and Their Mixture

Gaseous-phase photo-degradation for pure individual VOCs (acetone, toluene, and p-xylene) and their mixture was carried out in the continuous flow reactor system. The gas stream passed through the reactor at a flow rate of 5 L/min and contained 0.1 mol/m^3 pure acetone, toluene, or p-xylene, or 0.3 mol/m^3 of their mixture. The gas residence time was 72 s in the reactor. The experiment was run for 8 hr, and samples were collected at hourly intervals.

Both acetone and p-xylene in the mixed gas degraded at much lower rates than their pure individual gases under the same conditions, just as shown in Fig. 17. However, the opposite trend was observed for toluene. Toluene has an unsymmetrical structure, which leads to instability and promotes adsorption and degradation of pollutant molecules on the catalyst surface according to the L-H mechanism. In addition, the byproducts of acetone and p-xylene produced in the reaction could promote toluene degradation. In contrast, degradation of acetone and p-xylene in the mixed gas was reduced by competitive adsorption and catalysis of toluene. Among the pure gases and the mixture, acetone had the highest degradation efficiency. Furthermore, the efficiency of pure toluene degradation was lower than that of pure p-xylene degradation due to structural stability.

3.8. Effect of gas temperature

The effect of gas temperature on photo-catalytic degradation of gaseous toluene was investigated in the range of 25-50 °C (Fig. 18). The conditions were as follows: gas flow-rate of 1 L/min, relative humidity of 35%, irradiation time of 8 h, photo-catalyst of Ce-doped TiO_2, and initial concentration of 0.1 mol/m^3. Degradation efficiency of toluene gradually

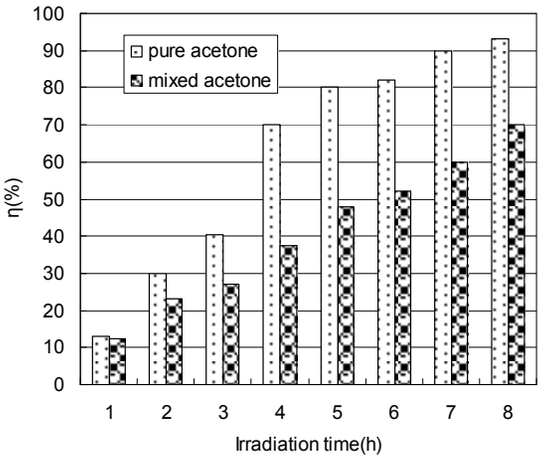

(a) Acetone

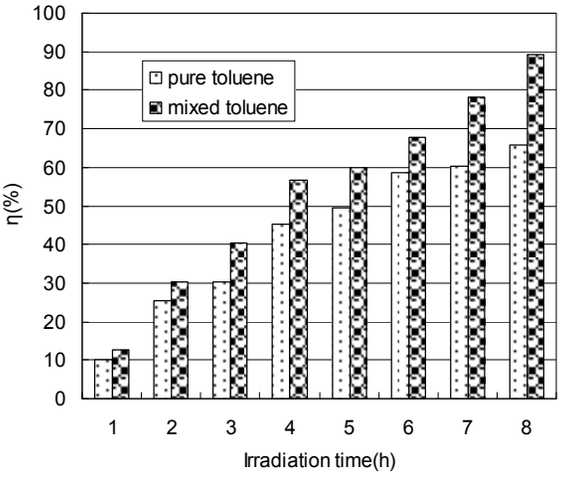

(b) Toluene

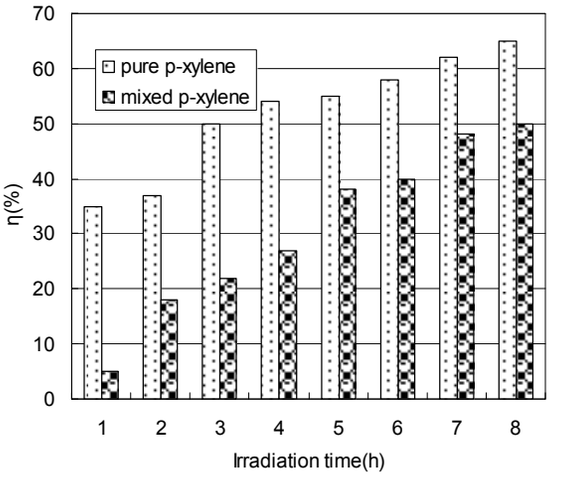

(c) P-xylene

Figure 17. Degradation with H_2O_2 of pure acetone, toluene, p-xylene, and their mixture.

increased when gas temperature was below 45 °C, but decreased at >45 °C. The increase in temperature would lead to the production of free radicals that could effectively collide with toluene molecules. Moreover, higher temperature may increase the oxidation rate of toluene at the interface. However, with increasing temperature, the adsorptive capacities of toluene on catalyst decreased, which led to the reduction of toluene removal efficiency.

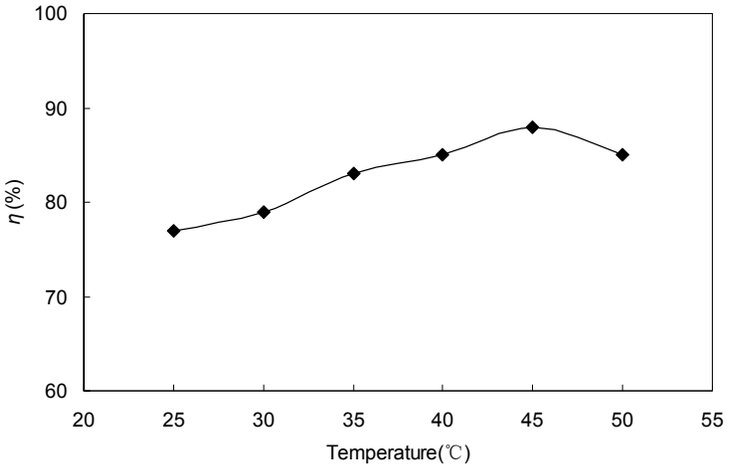

Figure 18. Effect of gas temperature on the photo-catalysis of toluene.

3.9. Effect of photo-catalyst amount

In photo-catalytic degradation of organic compounds, the optimal TiO_2 concentration depends mainly on both the nature of the compounds and the reactor geometry. In this work, the influence of TiO_2 amount on HCHO photo degradation was investigated. A set of gaseous experiments with different amount of TiO_2 from 0 to 100mg was carried out at the RH of 35% and the initial HCHO concentration of 0.1mg/m^3. The degradation rates of HCHO for different amount TiO_2 were presented in Fig. 19. The photo-catalytic degradation efficiency increased with increasing the amount of TiO_2 when TiO_2 amount was lower than 70mg. When the TiO_2 amount was more than 70mg, the photo-catalytic degradation efficiency was decreased. So 70mg of TiO_2 amount was the optional amount in our experiment. And the thickness of 70mg of TiO_2 amount was about 0.2mm.

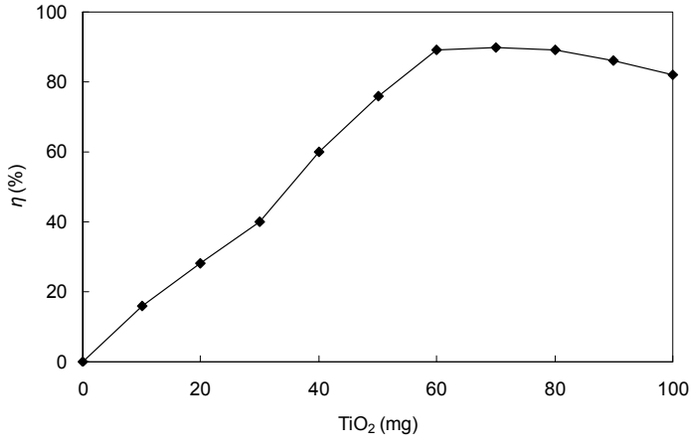

Figure 19. Effect of TiO_2 amount on HCHO degradation

At the same time, in our investigation, the effect of photo-catalyst concentration on the degradation of acetone in the gas flow was also analyzed in order to optimize the amount of TiO_2. Different concentrations (15-105 mg/L) of TiO_2 precursor sols were prepared by using different amounts of tetrabutyl orthotitanate. The conditions of the experiment were as follows: gas flow-rate of 1 L/min, relative humidity of 35%, Ce-doped TiO_2 as photo-catalyst, and irradiation time of 8 h. BET surface area of the synthesized samples was tested (see Table 2). The results showed that BET surface area increased with increasing photo-catalyst amount.

Sample concentration (mg/L)	15	30	45	60	75	90	105
BET (m^2/g)	50.2	66.2	68.2	72.2	78.3	88.8	88.9

Table 2. BET surface area for synthesized photo-catalyst.

Fig. 20 showed that the photo-catalytic degradation efficiency increased with increasing the amount of TiO_2. It was suggested that increasing efficiency was due to the increase of the surface area. It could be observed that the degradation efficiency increased with increasing the amount of the catalyst until it reached a plateau at 90-105 mg/L of TiO_2. This indicated that when the amount of TiO_2 was overdosed, the surface area was saturated, and then the intensity of UV was attenuated because of decreased light penetration and increased light scattering.

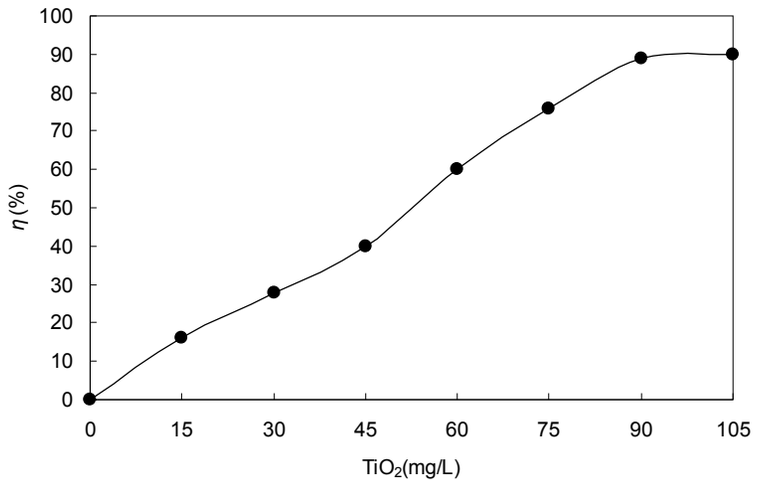

Figure 20. Effect of TiO_2 amount on the photo-catalysis of acetone.

3.10. Effect of relative humidity of air stream

The effect of relative humidity (0-60% RH) of air stream on HCHO decomposition was examined by adding water vapor to a fixed concentration of HCHO. TiO_2 photocatalyst was used in this experiment. Fig. 21 showed the experimental results at different relative humidity. The degradation rate increased with increasing relative humidity up to 35% and then started to decrease, which meant that 35% was the optimal humidity for photo-catalyst

process under the experimental conditions. When the reaction time was 120min, the highest removal efficiency of HCHO was 60.2% when RH was 35%.

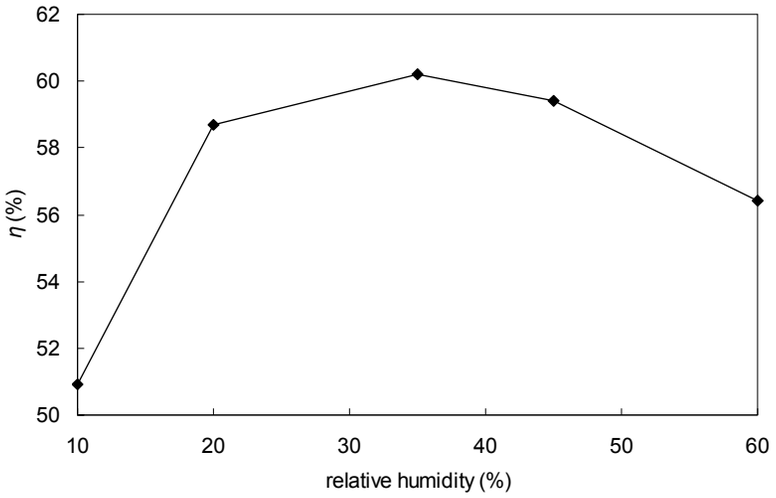

Figure 21. Effect of RH on decomposition of HCHO.

The enhancement of photo-catalytic reaction rate is frequently found in the presence of water vapor because hydroxyl groups or water molecules can behave as hole traps to form surface-adsorbed hydroxyl radicals. In photo-catalyst process, the hydroxyl radicals formed on the illuminated TiO_2 can not only directly attack HCHO molecules, but also suppress the electron-hole recombination. However, higher RH can be attributed to the competition for adsorption between HCHO and hydroxyl radicals, thus decrease the removal efficiency of HCHO.

3.11. Effect of oxygen concentration

The effect of oxygen concentration on HCHO degradation was presented in Fig. 22.

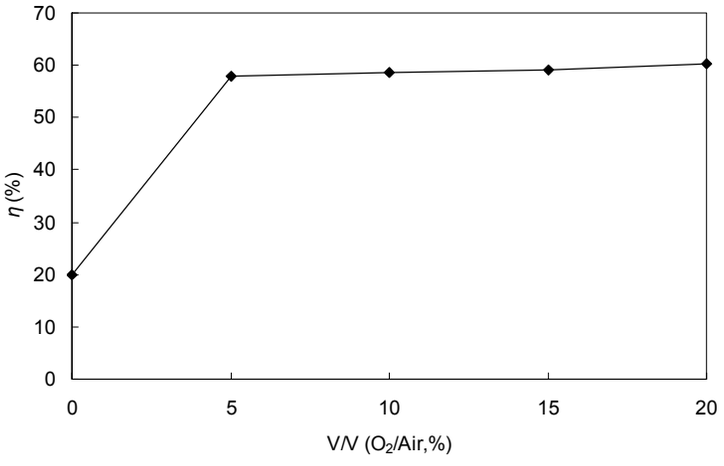

Figure 22. Effect of oxygen concentration on HCHO degradation.

The results corresponded to the initial concentration of 0.1mg/m^3, relative humidity of 35% and reaction time of 120min. It is obvious that oxidation rates for HCHO increased with increasing O_2 concentration under fixed conditions. As mentioned above, hydroxyl radical is an important factor to the HCHO photo-catalyst. At the same time, oxygen radical is also key factor for HCHO removal, which can react with HCHO on the TiO_2 surface and turn HCHO into CO_2 and H_2O.

3.12. Mechanism of photo-catalytic degradation of VOCs

The heterogeneous photo-catalytic process used in pollutant degradation involved the adsorption of pollutants on the surface sites, and the chemical reactions of converting pollutants into carbon dioxide and water. Activation of TiO_2 is achieved through the absorption of a photon (hv) with ultra-band energy from UV irradiation source. This results in the promotion of an electron (e−) from the valence band to the conduction band, with the generation of highly reactive positive holes (h+) in the valence band. This caused aggressive oxidation of the surface-adsorbed toxic organic pollutants and converts them into CO_2 and water.

In the degradation of toluene or p-xylene, the OH• radicals attack the phenyl ring of toluene or p-xylene, and some products, such as phenol, benzaldehyde or benzoic acid, may be produced during the reaction, and they were converted into CO_2 and H_2O at the end (Fig. 23). We could also observe that acetone was easily destructed to CO_2 and H_2O by photo-catalysts. By-products of toluene or p-xylene were detected by GC-MS, and involved phenol, benzaldehyde, aldehydes, alcohols, etc.

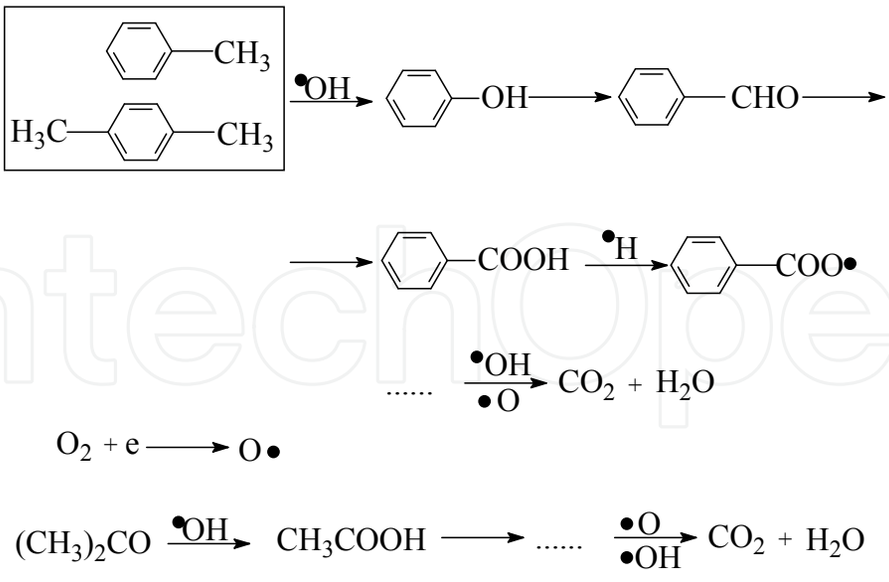

Figure 23. Suggested pathway for the photo-catalytic destruction of ATP.

The reaction rate constant (k) was chosen as the basic kinetic parameter for ATP since it was important in determination of VOCs photo-catalytic activity. The first order kinetic equation:

$$\ln\left(\frac{C_i}{C_o}\right) = k \times t + b \tag{7}$$

was used to fit experimental data in Fig. 24

where C_o is the concentration of ATP remaining in the solution at t, and C_i is the initial concentration at t = 0.

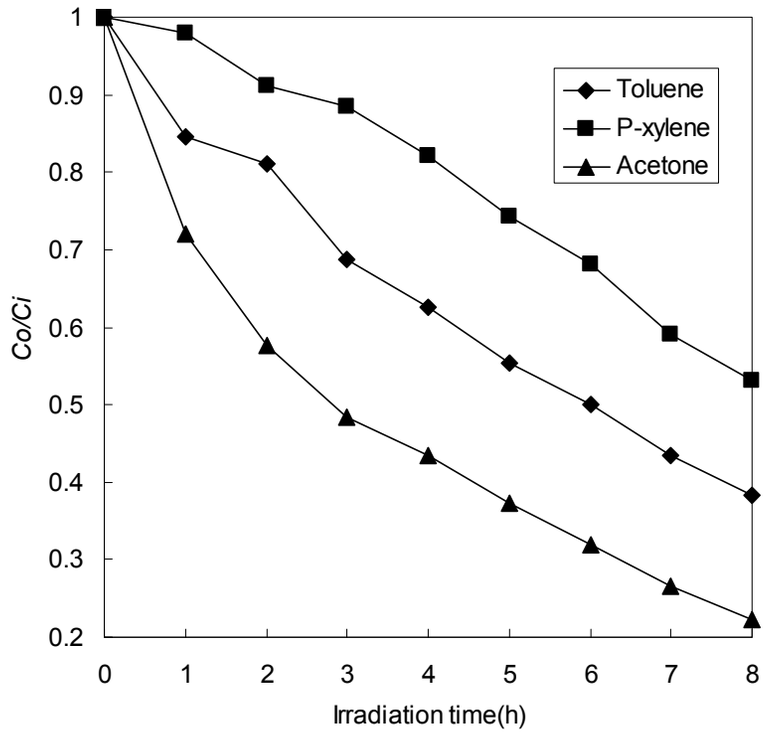

Figure 24. Kinetics of ATP degradation.

The variations in $\ln(C_i/C_o)$ as a function of irradiation time are given in Fig. 25. Reaction rate constant (k), linearity correlation coefficient (R) and intercept (b) data for the photo-catalytic destruction of ATP are exhibited in Table 3. The k of ATP could be ordered as follows: $k_{Acetone} > k_{Toluene} > k_{P\text{-}xylene}$, meaning that the decomposition capability of acetone was the best. The reason was probably due to molecular structure and molecular weight.

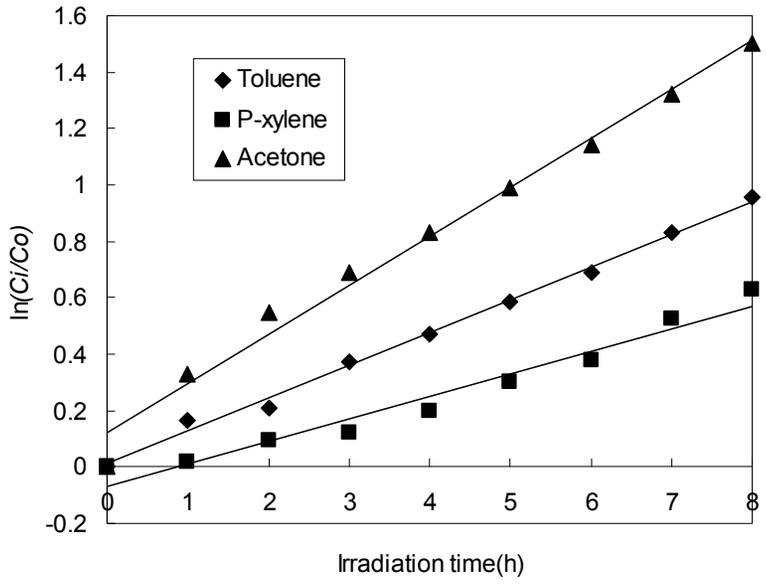

Figure 25. Relation between ln(C_i/C_o) and irradiation time, and linear fits for ATP.

	k (h^{-1})	R	b
Toluene	0.1165	0.998	0.0102
P-xylene	0.0797	0.980	-0.0668
Acetone	0.1742	0.993	0.12

Table 3. Values of k, R and b for the photo-catalytic destruction of ATP.

During the HCHO decomposition by photo-catalytic processing, formic acid was identified as the intermediate from the photo-degradation of formaldehyde. In our experiment, ion chromatography (IC) was used to determine the byproducts by sampling the gas products into distilled water. The result in this study showed that formic acid was also found. The probably pathway of HCHO destruction was shown in Fig. 26. The related reactions of HCHO destruction were shown with equations (8)-(21).

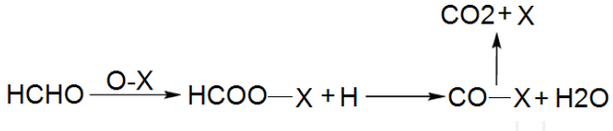

X : TiO_2, Ag/TiO_2 or Ce/TiO_2

Figure 26. Suggested pathway for the photo-catalytic destruction of HCHO

$$HCHO + e \longrightarrow H\bullet + CHO^- \quad (8)$$

$$HCHO + O\bullet \longrightarrow OH\bullet + CHO\bullet \quad (9)$$

$$HCHO + OH\bullet \longrightarrow H_2O + CHO\bullet \quad (10)$$

$$HCHO + OH\bullet \longrightarrow HCOOH + H\bullet \quad (11)$$

$$HCHO + H\bullet \longrightarrow H_2 + CHO\bullet \quad (12)$$

$$CHO\bullet + H\bullet \longrightarrow H_2 + CO \quad (13)$$

$$CHO\bullet + O_2 \longrightarrow CO_2 + OH\bullet \quad (14)$$

$$CHO\bullet + OH\bullet \longrightarrow H_2O + CO \quad (15)$$

$$CHO\bullet + HO_2\bullet \longrightarrow OH\bullet + H\bullet + CO_2 \quad (16)$$

$$CHO\bullet + O\bullet \longrightarrow OH\bullet + CO \quad (17)$$

$$CHO\bullet + O\bullet \longrightarrow H\bullet + CO_2 \quad (18)$$

$$HCOOH + OH\bullet \longrightarrow H_2O + H\bullet + CO_2 \quad (19)$$

$$CO + O\bullet \longrightarrow CO_2 \quad (20)$$

$$CO + OH\bullet \longrightarrow CO_2 + H\bullet \quad (21)$$

As mentioned in equation 7, k was the basic kinetic parameter for VOCs photo-catalytic activity. Fig. 27 showed the first order kinetic equation fitting the experimental data.

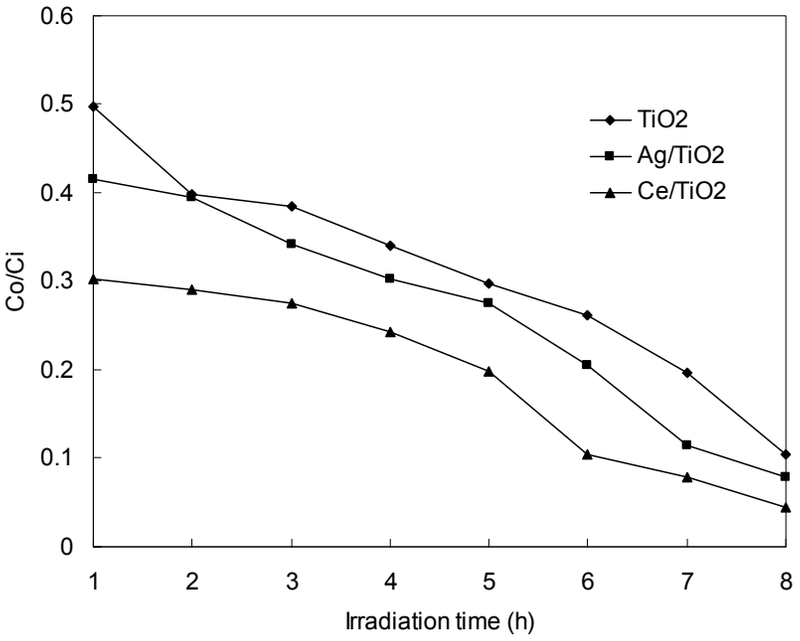

Figure 27. Kinetics of HCHO degradation.

The variations in $\ln(C_i/C_o)$ as a function of reaction time were given in Fig. 28. The reaction rate constant for TiO_2、Ag/TiO_2、Ce/TiO_2 were 0.1871、0.2302、0.2724, respectively, which meant that Ce/TiO_2 had the best photo-catalytic abilities among the catalysts.

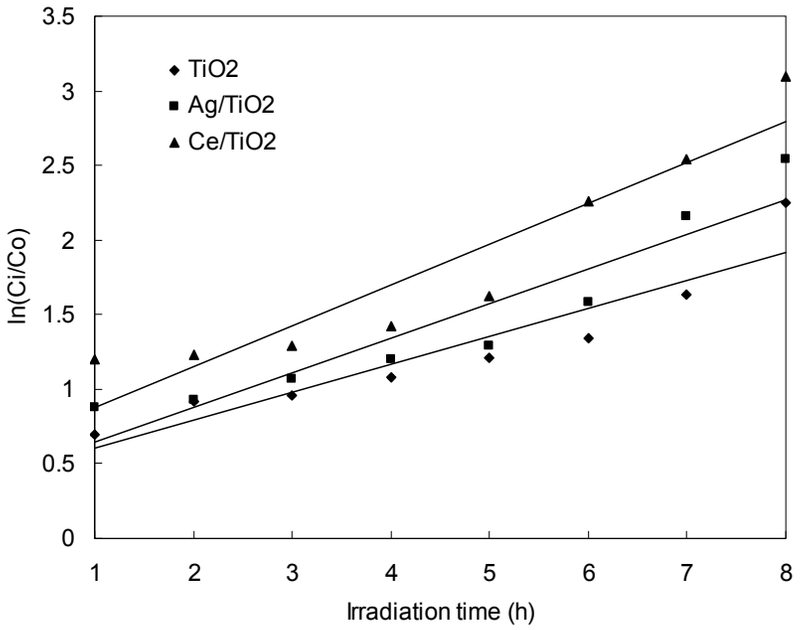

Figure 28. Relationship between $\ln(C_i/C_o)$ and reaction time.

4. Conclusion

In this chapter, nano-structured TiO_2, Ag-TiO_2 and Ce-TiO_2 thin films coated on glass springs were prepared by sol-gel method at room temperature. Toluene, p-xylene, acetone and formaldehyde were chosen as the model VOCs, the photo-catalytic degradation characters of them by TiO_2/UV, TiO_2/doped Ag/UV and TiO_2/doped Ce/UV was tested and compared. The effects of doped Ag/Ce ions, hydrogen peroxide, initial concentration, gas temperature, relative humidity of air stream, oxygen concentration, gas flow rate, UV light wavelength and photo-catalyst amount on decomposition of the pollutants by TiO_2/UV were analyzed simultaneously. Furthermore, the mechanism of titania-assisted photo-catalytic degradation was analyzed, and the end product of the reaction using GC-MS analysis was also performed.

Results were as follows: (1) Characterization of this film by SEM and XRD showed it consisted of nanoparticles, and the crystalline phase was anatase. (2) Doped Ag or Ce ions could enhance the photo-catalyst ability. The degradation character of the photo-catalyst was in the order Ce-TiO_2 > Ag-TiO_2 > TiO_2. (3) Hydrogen peroxide could promote the activation of catalyst, and toluene & p-xylene degradation rate with hydrogen peroxide was higher than that without it. The final degradation rates of toluene and p-xylene using H_2O_2 were up to 97.1 and 95.4% after 8 h, respectively. (4) The photo-catalytic degradation rates decreased with increasing VOCs initial concentration. Acetone was easiest to be destructed,

while p-xylene was difficult to remove from gas flow. (5) The degradation efficiency gradually increased with gas temperature and 45 °C had the best removal efficiency. (6) 35% was the optimal humidity for photo-catalyst process under the experimental conditions. (7) Higher concentration of oxygen was better for HCHO removal. (8) The flow rate greatly influenced the degradation rate. For acetone and toluene, the degradation rate was highest with a flow rate of 3 L/min. For p-xylene, the degradation rate was highest when the flow rate was 7 L/min. The highest degradation rates for acetone, toluene and p-xylene were 77.7 %, 61.9 % and 55 %, respectively. (9) Illumination using a 254 nm light source was better than 365 nm. (10) The photo-catalytic degradation efficiency increased with increasing the amount of TiO_2 when TiO_2 amount was lower than 70mg. (11) In the gas mixture, acetone and p-xylene had much lower degradation rates than for their pure counterparts. The opposite trend was observed for toluene. Among acetone, toluene and p-xylene, the removal efficiency of acetone was highest both when pure and as a part of the gas mixture. (12) The photo-catalytic process used in pollutant degradation involved the adsorption of pollutants on the surface sites, and chemical reactions of converting pollutant into CO_2 and H_2O at the end. By-products of toluene or p-xylene were detected by GC-MS analysis, and involved phenol, benzaldehyde, aldehydes, alcohols, etc. The reaction rate constant (k) of ATP was sequenced $k_{Acetone}>k_{Toluene}>k_{P\text{-}xylene}$, meaning that the decomposition capability of acetone was the best, probably due to molecular structure and molecular weight. Formic acid was the main byproduct during the decomposition of HCHO. The reaction rate constant (k) of TiO_2、Ag/TiO_2、Ce/TiO_2 was sequenced $k_{Ce/TiO2}>k_{Ag/TiO2}>k_{TiO2}$, meaning that Ce/TiO_2 had the best photo-catalytic abilities among the catalysts.

Author details

Wenjun Liang, Jian Li and Hong He
College of Environmental and Energy Engineering,
Beijing University of Technology, Beijing, China

Acknowledgement

This work was supported by National high technology research and development program of China (2011AA03A406) and Project of Beijing Municipal Education Commission (KM201110005011).

5. References

Akira F., Tata N.R., Donald A. (2000). Titanium dioxide photocatalysis, Journal of Photochemistry and Photobiology C: Photochemistry Reviews, Vol. 1,pp.1–21.

Alberici, R.M., Jardim, W.E. (1997). Photocatalytic destruction of VOCs in the gas-phase using titanium dioxide. Appl. Catal. B-Environ., Vol.14, pp. 55-68.

Ao C.H., Lee S.C., Yu J.Z., Xu J.H. (2004). Photodegradation of formaldehyde by photocatalyst TiO2: effects on the presences of NO, SO2 and VOCs. Appl. Catal. B., Vol.54, pp.41–50.

Biard, P.F.; Bouzaza, A.; Wolbert, D. (2007). Photocatalytic Degradation of Two Volatile Fatty Acids in an Annular Plug-Flow Reactor; Kinetic Modeling and Contribution of Mass Transfer Rate. Environ. Sci. Technol., Vol.41, pp.2908-2914.

Boulamanti, A. K.; Philippopoulos, C. J. (2008). Photocatalytic degradation of methyl tert-butyl ether in the gas-phase: A kinetic study. J. Hazard Mater., Vol.160, pp. 83-87.

Boulamanti, A.K.; Korologos, C.A.; Philippopoulos, C.J. (2008). The rate of photocatalytic oxidation of aromatic volatile organic compounds in the gas-phase. Atmos. Environ., Vol.42, pp.7844-7850.

Bouzaza A., Vallet C., Laplanche A. (2006) Photocata-lytic degradation of some VOCs in the gas phase using an an-nular flow reactor. Determination of the contribution of mass transfer and chemical reaction steps in the photodegradation process. J. Photochem. Photobiol. A: Chem. Vol.177, pp.212-217.

Carp O., Huisman C.L., Reller A. (2004). Photoinduced reactivity of titanium dioxide. Prog. Solid State Chem., Vol.32, pp. 33-177.

Chatterjee D., Dasgupta S. (2005) Visible light induced photocatalytic degradation of organic pollutants. J. Photo-chem. Photobiol. C. Vol.6, pp.186-205.

Chen F., Pehkonen S.O., Ray M.B. (2002) Kinetics and mechanisms of UV-photodegradation of chlorinated organics in the gas phase. Water Res. Vol.36, pp.4203-4214.

Chen F., Yang Q., Pehkonen S.O., Ray M.B. (2004) Modeling of gas phase photodegradation of chlorinated VOCs. J. Air Waste Manage Assoc. Vol.54, pp.1281-1292.

Chen, X.B.; Mao, S.S. (2007). Titanium Dioxide Nanomaterials: Synthesis, Properties, Modifications, and Applications. Chem. Rev., Vol.107, pp. 2891-2959.

Collins J.J., Ness R., Tyl R.W., Krivanek N., Esmen N.A., Hall T.A. (2001). A Review of Adverse Pregnancy Outcomes and Formaldehyde Exposure in Human and Animal Studies. Regul. Toxicol. Pharm., Vol.34, pp.17-34.

Fujishima A., Zhang X.T. (2006). Titanium dioxide photocatalysis: present situation and future approaches, C. R. Chimie, Vol.9,pp.750–760.

Futamura S., Zhang A., Einaga H., Kabashima H. (2002) Involvement of catalyst materials in nonthermal plasma chemical processing of hazardous air pollutants. Catal. Today. Vol.72, pp.259-265.

González A. S., Martínez S. S. (2008) Study of the sono-photocatalytic degradation of basic blue 9 industrial textile dye over slurry titanium dioxide and influencing factors. Ultrason. Sonochem. Vol.15, pp. 1038-1042.

Hirakawa, T.; Koga, C.;Negishi, N.; Takeuchi, K.; Matsuzawa, S. (2009). An approach to elucidating photocatalytic reaction mechanisms by monitoring dissolved oxygen: Effect of H2O2 on photocatalysis, Appl Catal B: Environ., Vol.87, pp. 46-55.

Holzer F., Roland U., Kopinke F.D. (2002) Combination of non-thermal plasma and heterogeneous catalysis for oxidation of volatile organic compounds Part 1. Accessibility of the intra-particle volume. *Appl. Catal. B: Environ*. Vol.38, pp.163-181.

http://www.epa.gov/iaq/voc.html

Hu, Q.H.; Zhang, C.L.; Wang, Z.R.; Chen, Y.; Mao, K.H.; Zhang, X.Q.; Xiong, Y.L.; Zhu, M.J. (2008). Photodegradation of methyl tert-butyl ether (MTBE) by UV/H_2O_2 and UV/TiO_2. *J. Hazard Mater.,* Vol.154, pp.795-803.

Jacoby W.A., Blake D.M., Noble R.D., Koval C.A. (1995). Kinetics of the Oxidation of Trichloroethylene in Air via Heterogeneous Photocatalysis. *J. Catal*., Vol.157, pp.87-96.

Jing L.Q., Xu Z.L., Sun X.J., Shang J., Cai W.M. (2001). The surface properties and photocatalytic activities of ZnO ultrafine particles. *Appl. Surf. Sci.*, Vol.180, pp.308-314.

Kecske´s T., Rasko´J., Kiss J. (2004). FTIR and mass spectrometric studies on the interaction of formaldehyde with TiO_2 supported Pt and Au catalysts. *Appl. Catal. A*, Vol.273, pp.55-62.

Kim, S.B.; Hong, S.C. (2002). Kinetic study for photocatalytic degradation of volatile organic compounds in air using thin film TiO_2 photocatalyst. *Appl Catal B: Environ*., Vol. 35, pp.305-315.

Li F.B., Li X.Z., Hou M.F., Cheah K.W., Choy W.C.H. (2005) Enhanced photocatalytic activity of Ce^{3+}-TiO_2 for 2-mercaptobenzothiazole degradation in aqueous suspension for odour control. *Appl. Catal. A: Gen*. Vol.285, pp.181-189.

Li, D.; Haneda, H.; Hishita, S.; Ohashi, N. (2005). Visible-light-driven nitrogen-doped TiO_2 photocatalysts: effect of nitrogen precursors on their photocatalysis for decomposition of gas-phase organic pollutants. *Mater. Sci. Eng. B.*, Vol.117, pp. 67-75.

Li, F.B.; Li, X.Z.; Ao, C.H.; Lee, S.C.; Hou, M.F. (2005).Enhanced photocatalytic degradation of VOCs using Ln^{3+}–TiO_2 catalysts for indoor air purification. *Chemosphere*, Vol.59, pp.787-800.

Lin L., Zheng R.Y., Xie J.L., Zhu Y.X., Xie Y.C. (2007). Synthesis and characterization of phosphor and nitrogen co-doped titania. *Appl. Catal. B.*, Vol.76, pp.196-202.

Liu H.M., Lian Z.W., Ye X.J., Shangguan W.F. (2005). Kinetic analysis of photocatalytic oxidation of gas-phase formaldehyde over titanium dioxide. *Chemosphere*, Vol.60, pp.630-635.

Liu T.X., Li F.B., Li X.Z. (2008). TiO_2 hydrosols with high activity for photocatalytic degradation of formaldehyde in a gaseous phase. *J. Hazard. Mater.*, Vol.152, pp.347-355.

Lu Y.W., Wang D.H., Ma C.F., Yang H.C. (2010). The effect of activated carbon adsorption on the photocatalytic removal of formaldehyde. *Building and Environment*, Vol.45, pp.615–621.

Mohseni, M. (2005). Gas phase trichloroethylene (TCE) photooxidation and byproduct formation: photolysis vs. titania/silica based photocatalysis. *Chemosphere*, Vol.59, pp. 335-342.

Obee, T.N. (1995). TiO_2 Photocatalysis for Indoor Air Applications: Effects of Humidity and Trace Contaminant Levels on the Oxidation Rates of Formaldehyde, Toluene, and 1, 3-Butadiene. *Environ. Sci. Technol.*, Vol.29, pp.1223-1231.

Ogata A., Einaga H., Kabashima H., Futamura S., Kushi-yama S., Kim H. H. (2003) Effective combination of nonthermal plasma and catalysts for decomposition of benzene in air. *Appl. Catal. B: Environ*. Vol.46, pp.87-95.

Ohno T., Tsubota T., Nakamura Y., Sayama K.(2005). Preparation of S, C cation-codoped $SrTiO_3$ and its photocata-lytic activity under visible light. *Appl. Catal. A.*, Vol.288, pp.74-79.

Ohtani B. (2010). Photocatalysis A to Z—What we know and what we do not know in a scientific sense, *Journal of Photochemistry and Photobiology C: Photochemistry Reviews,* Vol.11, pp.157–178.

Olmez T. (2008) Photocatalytic Treatment of phenol with visible light irradiation. *Fresen. Environ. Bull*. Vol.17, pp.1796-1802.

P´erez, M.; Torrades, F.; Garc´ıa-Hortal, J.A.; Dom`enech, X.; Peral, J. (2002). Removal of organic contaminants in paper pulp treatment effluents under Fenton and photo-Fenton conditions. *Appl. Catal. B: Environ.*, Vol.36, pp.63-74.

Parmar, G.R., Rao N.N. (2009). Emerging Control Technologies for Volatile Organic Compounds, *Critical Reviews in Environmental Science and Technology*, Vol.39, pp.41-78.

Sakthivel, S.; Kisch, H. (2003). Photocatalytic and photoelectrochemical properties of nitrogen-doped titanium dioxide. *Chem. Phys. Chem.*, Vol.4, pp. 487-490.

Sano T., Negishi N., Takeuchi K., Matsuzawa S. (2004). Degradation of toluene and acetaldehyde with Pt-loaded TiO_2 catalyst and parabolic trough concentrator. *Solar Energy*, Vol.77, pp.543-552.

Shan G.B., Yan S., Tyagi R.D., Surampalli R.Y., Zhang T.C. (2009). Applications of Nanomaterials in Environmental Science and Engineering: Review, *Practice Peri-odical of Hazardous, Toxic, and Radioactive Waste Management,* Vol.13, pp.110-119.

Shang J., Du Y.G., Xu Z.L. (2002). Photocatalytic oxidation of heptane in the gas-phase over TiO_2.*Chemosphere,* Vol.46, pp.93-99.

Shiraishi F., Yamaguchi S., Ohbuchi Y. (2003). A rapid treatment of formaldehyde in a highly tight room using a photocatalytic reactor combined with a continuous adsorption and desorption apparatus. *Chem. Eng. Sci.*, Vol.58, pp.929-934.

Sleiman, M.; Conchon, P.; Ferronato, C.; Chovelon, J.M. (2009). Photocatalytic oxidation of toluene at indoor air levels (ppbv): Towards a better assessment of conversion, reaction intermediates and mineralization. *Appl Catal B: Environ.*, Vol.86, pp.159-165.

Somekawa S., Kusumoto Y., Ikeda M., Ahmmad B., Horie Y. (2008). Fabrication of N-doped TiO_2 thin films by laser ablation method: Mechanism of N-doping and evaluation of the thin films. *Catal. Commun.*, Vol.9, pp.437-440.

Song L., Qiu R.L., Mo Y.Q., Zhang D.D., Wei H., Xiong Y. (2007). Photodegradation of phenol in a polymer-modified TiO2 semiconductor particulate system under the irradiation of visible light. *Catal. Commun.*, Vol.8, pp.429-433.

Sun R.B., Xi Z.G., Chao F.H., Zhang W., Zhang H.S., Yang D.F. (2007) Decomposition of low-concentration gas-phase toluene using plasma-driven photocatalyst reactor. *Atmos. Environ*. Vol.41, pp.6853-6859.

Tanada S., Kawasaki N., Nakamura T., Araki M., Isomura M. (1999). Removal of Formaldehyde by Activated Carbons Containing Amino Groups. *J. Colloid. Interf. Sci.*, Vol.214, pp.106-108.

Tokumura, M.; Nakajima, R.; Znad, H. T.; Kawase, Y. (2008). Chemical absorption process for degradation of VOC gas using heterogeneous gas–liquid photocatalytic oxidation: Toluene degradation by photo-Fenton reaction. *Chemosphere*, Vol.73, pp. 768-775.

Venkatachalam N., Palanichamy M., Arabindoo B., Mu-rugesan V. (2007). Alkaline earth metal doped nanoporous TiO_2 for enhanced photocatalytic mineralisation of bisphenol-A. *Catal. Commun.*, Vol.8, pp.1088-1093.

Vincenzo A., Marta L., Leonardo P., Javier S. (2006). The combination of heterogeneous photocatalysis with chemical and physical operations: A tool for improving the photoprocess performance, *Journal of Photochemistry and Photobiology C: Photochemistry Reviews,* Vol.7,pp.127–144.

Wang J.H., Ray M.B. (2000) Application of ultraviolet photooxidation to remove organic pollutants in the gas phase. *Sep. Purif. Technol*. Vol.19, pp.11-20.

Wang Y.Y., Zhou G.W., Li T.D., Qiao W.T., Li Y.J. (2009) Catalytic activity of mesoporous $TiO_{2-x}N_x$ photocatalysts for the decomposition of methyl orange under solar simulated light. *Catal. Commun*. Vol.10, pp.412–415.

Wang, X.Q.; Zhang, G.L.; Zhang, F.B.; Wang, Y. (2006). Study integration about Photocatalytic degradation of gaseous benzene in atmosphere by using TiO_2 photocatalyst. *Chemical Research and Application*, Vol.18, pp.344-348.

Wu C.D., Xu H., Li H.M., Chu J.Y., Yan Y.S., Li C.S. (2007) Photocatalytic decolorization of methylene blue via Ag-deposited BiVo(4) under UV-light irradiation. *Fresen. Environ. Bull*. Vol.16, pp. 242-246.

Xu Y.H., Chen H.R., Zeng Z.X., Lei B. (2006). Investigation on mechanism of photocatalytic activity enhancement of nanometer cerium-doped titania. *Appl. Surf. Sci.*, Vol.252, pp.8565–8570.

Yang S.X., Zhu W.P., Jiang Z.P., Chen Z.X., Wang J.B. (2006). The surface properties and the activities in catalytic wet air oxidation over CeO_2–TiO_2 catalysts. *Appl. Surf. Sci.*, Vol.252, pp.8499-8505.

Yang X., Xu L.L., Yu X.D., Guo Y.H. (2008) One-step preparation of silver and indium oxide co-doped TiO_2 photo-catalyst for the degradation of rhodamine B. *Catal. Commun.* Vol.9, pp.1224-1229.

Yi Z., Wei W., Lee S., Gao J.H. (2007). Photocatalytic performance of plasma sprayed Pt-modified TiO_2 coatings under visible light irradiation. *Catal. Commun.*, Vol.8, pp.906-912.

Yu J.C., Yu J.G., Ho W.K., Zhang L.Z. (2001). Preparation of highly photocatalytic active nano-sized TiO_2 particles via ultrasonic irradiation. *Chem. Commun.*, Vol.19, pp.1942-1943.

Yu J.G., Yu J.C., Cheng B., Hark S.K., Iu K. (2003). The effect of F−-doping and temperature on the structural and textural evolution of mesoporous TiO_2 powders. *J. Solid State Chem.*, Vol.174, pp.372-380.

Zhang C.B., He H. (2007). A comparative study of TiO_2 supported noble metal catalysts for the oxidation of formaldehyde at room temperature. *Catalysis Today*, Vol.126, pp.345–350.

Zhang C.B., He H., Tanaka K.I. (2005). Perfect catalytic oxidation of formaldehyde over a Pt/TiO_2 catalyst at room temperature. *Catal. Commun.*, Vol.6, pp.211-214.

Zhang C.B., He H., Tanaka K.I. (2006). Catalytic performance and mechanism of a Pt/TiO_2 catalyst for the oxidation of formaldehyde at room temperature. *Appl. Catal. B.*, Vol.65, pp.37–43.

Zhang, P.Y.; Liang, F.Y.; Yu, G.; Chen, Q.; Zhu, W.P. (2003). A comparative study on decomposition of gaseous toluene by O_3/UV, TiO_2/UV and O_3/TiO_2/UV. *J. Photoch. Photobio. A.*, Vol.156, pp.189-194.

Zou, L.D.; Luo, Y.G.; Hooper, M.; Hu, Eric. (2006). Removal of VOCs by photocatalysis process using adsorption enhanced TiO_2-SiO_2 catalyst. *Chem. Eng. Process.*, Vol.45, pp.959-964.

Zuo G.M., Cheng Z.X., Chen H., Li G.W., Miao T. (2006) Study on photocatalytic degradation of several volatile or-ganic compounds. *J. Hazard. Mater.* Vol.128, pp.158-163.